

# Crystal structures and solid-state CPMAS $^{13}\text{C}$ NMR correlations in luminescent zinc(II) and cadmium(II) mixed-ligand coordination polymers constructed from 1,2-bis(1,2,4-triazol-4-yl)ethane and benzenedicarboxylate<sup>†</sup>

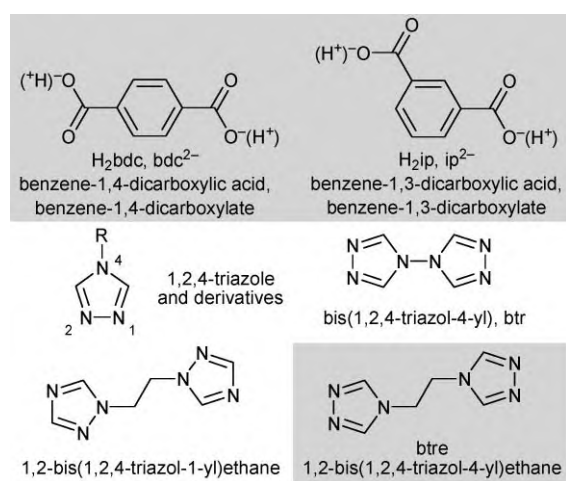
Hesham A. Habib,<sup>a</sup> Anke Hoffmann,<sup>b</sup> Henning A. Höppe<sup>a</sup> and Christoph Janiak<sup>\*a</sup>

The hydrothermal reaction of  $\text{M}(\text{NO}_3)_2 \cdot 4\text{H}_2\text{O}$  ( $\text{M} = \text{Zn}$  and  $\text{Cd}$ ) with benzene-1,4-dicarboxylic acid ( $\text{H}_2\text{bdc}$ ) or benzene-1,3-dicarboxylic acid ( $\text{H}_2\text{ip}$ ) and 1,2-bis(1,2,4-triazol-4-yl)ethane ( $\text{btre}$ ) produced the mixed-ligand coordination polymers (MOFs)  $\{\text{[Zn}_2(\mu_2\text{-bdc})_2(\mu_4\text{-btre})]\}$  (**1**),  $\{\text{[Cd}_2(\mu_4\text{-bdc})(\mu_4\text{-btre})_2]\}(\text{NO}_3)_2 \cdot \text{H}_2\text{O}$  (**2**) and  $\{\text{[Zn}_2(\mu_3\text{-ip})_2(\mu_2\text{-btre})\}(\text{H}_2\text{O})_2\} \cdot 2\text{H}_2\text{O}$  (**3**). The compounds, characterized by single-crystal X-ray diffraction, X-ray powder diffraction, solid-state cross-polarization (CP) magic-angle-spinning (MAS)  $^{13}\text{C}$  NMR and thermoanalysis, feature 3D metal–organic frameworks for **1** and **2** and 2D double layers which are connected through hydrogen bonds from the aqua ligands for **3**. The CPMAS  $^{13}\text{C}$  NMR spectra picture the symmetry-independent (unique) C atoms and the bdc/ip-to-btre ligand ratio in agreement with the crystal structures. The zinc and cadmium coordination polymers **1–3** show a strong bluish fluorescence upon excitation with UV light (the free btre ligand is non-luminescent).

## Introduction

Metal–organic frameworks (MOFs) or coordination polymers attract much attention in recent years because of topology and potential applications in catalysis, adsorption (gas storage), luminescence, magnetism, etc.<sup>1–4</sup> Luminescent stable metal–organic coordination polymers have been an active research area for decades because of their potential applications in materials science.<sup>1,5,6</sup> Mixed-ligand coordination polymers<sup>7,8</sup> based on a luminescent and a non-luminescent ligand should allow for a dilution of the luminescent centers to avoid concentration quenching effects. Multi-carboxylate ligands with suitable spacers, especially benzoic acid-based ligands and also the 1,2,4-triazole ligand and its derivatives<sup>9</sup> are frequent choices for metal–organic networks.<sup>1</sup> Benzenedi- or -tricarboxylates can exhibit luminescence in coordination polymers with metal nodes such as zinc or cadmium.<sup>5,10</sup> Benzene-1,4-dicarboxylate,<sup>11</sup> ( $\text{bdc}^{2-}$ , terephthalate, Scheme 1) with a  $180^\circ$  angle between the two carboxylic groups, can form short bridges *via one* carboxylato end, thereby simultaneously linking up to four metal ions within a metal–metal separation of about  $11\text{ \AA}$ ,<sup>12–15</sup> or it forms long bridges *via* the benzene ring, leading to a great variety of structures.<sup>16,17</sup> Also benzene-1,3-dicarboxylate, ( $\text{ip}^{2-}$ , isophthalate)<sup>18</sup> in which the two carboxylate moieties are rigidly predisposed at  $120^\circ$  (Scheme 1), is an equally good oxygen

donor for building metal–organic networks. The 1,2,4-triazole ligand and its 4-substituted derivatives can be used to obtain linear coordination polymers based on its bridging function, e.g., with  $\text{Cu}^{2+}$ ,<sup>19</sup>  $\text{Zn}^{2+}$ ,<sup>20</sup>  $\text{Cd}^{2+}$ ,<sup>21</sup> together with a wide variety of molecular polynuclear complexes.<sup>22</sup> The *N*1,*N*2-bridging mode of 1,2,4-triazole or triazolate (Scheme 1) constitutes a short ligand bridge between metal atoms which is a prerequisite for stronger magnetic coupling between paramagnetic metal centers.<sup>1</sup> Surprisingly, with the related 4,4'-bis(1,2,4-triazol-4-yl) ligand (abbreviated as btr) this *N*1,*N*2-bridging coordination mode has only been observed recently with  $\text{Cu}(\text{II})$ .<sup>23</sup> The btr ligand links transition metal(II) ions, using only one nitrogen atom from each 1,2,4-triazole ring, to one-,<sup>24,25</sup> two-, and three-dimensional<sup>26–28</sup> networks. With alkylene spacers between the two 1,2,4-triazole



<sup>a</sup>Institut für Anorganische und Analytische Chemie, Universität Freiburg, Albertstr. 21, 79104, Freiburg, Germany. E-mail: janik@uni-freiburg.de; Fax: +49 761 2036147; Tel: +49 761 2036127

<sup>b</sup>Institut für Makromolekulare Chemie, Universität Freiburg, Stefan-Meier-Str. 31, D-79104, Freiburg, Germany. E-mail: anke.hoffmann@makro.uni-freiburg.de; Fax: +49 761 2036306; Tel: +49 761 2036314

† Electronic supplementary information (ESI) available: X-Ray powder diffractograms, thermogravimetric analyses, C–H $\cdots$ O/N and O–H $\cdots$ O/N hydrogen bonds for **1–3**. CCDC reference numbers 695986, 695987 and 695988 for **1–3**, respectively. For ESI and crystallographic data in CIF or other electronic format see DOI: 10.1039/b812670d

**Scheme 1** Ligands relevant to this work. The grey underlined ligands are synthetically used in this work.

rings, the resulting ligand acquires more flexibility. Therefore, we selected 1,2-bis(1,2,4-triazol-4-yl)ethane (abbreviated as btre).<sup>29</sup> This btre ligand, which must not be mistaken with the 1,2-bis(1,2,4-triazol-1-yl)ethane ligand,<sup>30</sup> has been scarcely used in metal-complex or MOF synthesis.

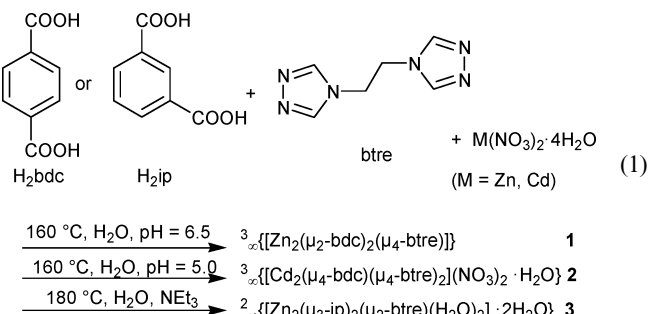
A CSD search<sup>31</sup> gave  $^2\{\text{M}(\text{NCS})_2(\mu_2\text{-btre})_2(\text{NCS})_2\}$  ( $\text{M} = \text{Fe}, \text{Co}$ )<sup>32</sup>,  $^3\{[\text{Cu}_3(\mu_4\text{-btre})_2(\mu_3\text{-btre})_4(\text{H}_2\text{O})_2]_2(\text{ClO}_4)_2\cdot 2\text{H}_2\text{O}\}$ <sup>33</sup>,  $^3\{[\text{Ni}_3(\mu_3\text{-btc})_2(\mu_4\text{-btre})_2(\mu\text{-H}_2\text{O})_2]\cdot 22\text{H}_2\text{O}\}$ ,  $^3\{[\text{Ni}_3(\mu_2\text{-btc})_2(\mu_4\text{-btre})_2(\mu\text{-H}_2\text{O})_2(\text{H}_2\text{O})_2]\cdot 4\text{H}_2\text{O}\}$ ,  $^3\{[\text{Zn}_3(\mu_4\text{-btc})_2(\mu_4\text{-btre})(\text{H}_2\text{O})_2]\cdot 2\text{H}_2\text{O}\}$  and  $^3\{[\text{Zn}_3(\mu_6\text{-btc})_2(\mu_4\text{-btre})]\cdot 0.67\text{H}_2\text{O}\}$ <sup>7</sup> as the only examples.

Herein, we report the structures, structure-CPMAS-NMR correlation and luminescence of mixed-ligand coordination networks of  $\text{bdc}^{2-}$  or  $\text{ip}^{2-}$  and btre with zinc and cadmium.

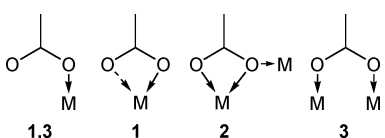
## Results and discussion

### Synthesis

Hydrothermal treatments of metal nitrates with 1,2-bis(1,2,4-triazol-4-yl)ethane (btre) and benzene-1,4-dicarboxylic acid ( $\text{H}_2\text{bdc}$ ) or benzene-1,3-dicarboxylic acid ( $\text{H}_2\text{ip}$ ) yield the mixed-ligand coordination polymers **1** to **3** (eqn (1)). Complete deprotonation of  $\text{H}_2\text{ip}$  is achieved through the addition of triethylamine ( $\text{NEt}_3$ ).



The dicarboxylate ligands coordinate towards the metal atoms in **1–3** as shown in Scheme 2.



**Scheme 2** The four types of coordination modes of the carboxylate groups of bdc and ip ligands in compounds **1–3**.

The vibrational modes for carboxylate groups, substituted benzene and triazole rings confirm the presence of deprotonated bdc, ip and btre ligands in compounds **1–3**. The absence of bands at  $1730\text{--}1690\text{ cm}^{-1}$  for  $-\text{COOH}$  is indicative of fully deprotonated  $\text{bdc}^{2-}$  and  $\text{ip}^{2-}$  ligands in **1–3**. The extensive hydrogen-bonding network in the crystal structure of **3** (Table S1, Fig. S9 in ESI†) is indicated through the  $\delta$ - and  $\gamma$ -vibrational modes between  $880$  and  $1350\text{ cm}^{-1}$ .<sup>34</sup>

### Thermal stability

A sample of compound **1** shows the first weight loss in the TGA (Fig. S4 in ESI†) in the temperature range  $260\text{--}370\text{ °C}$  which corresponds to the removal of one btre (or bdc) ligand (obs. 25.0,

calcd. 26.3%). A continuing weight loss from  $370$  to  $600\text{ °C}$  matches with a complete loss of the remaining 2 bdc or btre + bdc ligands (obs. 54.8, calcd. 52.6%). A sample of compound **2** shows the first weight loss in the temperature range  $80\text{--}160\text{ °C}$  in the TGA (Fig. S5 in ESI†) or up to  $110\text{ °C}$  in the TGA-IR-MS which corresponds to the removal of the crystal water molecule ( $m/z = 17$  and  $18$  in MS,  $\text{H}_2\text{O}$  bands in IR; TGA obs. 2.5, TGA-IR-MS obs. 1.8%, calcd. 2.1%). The weight loss seems to continue mainly with the removal of the btre molecules. In the range  $350\text{--}420\text{ °C}$  the TGA-IR shows bands for nitrile,  $\text{HCN}$ ,  $\text{NH}_3$  and/or hydrazine and  $\text{CO}_2$  which matches with the TGA-IR of the free btre ligand. From  $400\text{ °C}$  on the MS shows  $m/z = 50, 52, 76, 78, 79, 103, 104$  which come from typical aromatic fragments (e.g.  $104 = [\text{C}_6\text{H}_4\text{-CO}]^+$ ) and are derived from  $\text{bdc}^{2-}$ . A remaining 32.4% (TGA) or 28% (TGA-IR-MS) suggests the formation of  $\text{CdO}$  (calcd. 29.9%). A sample of compound **3** shows the first weight loss in the temperature range  $80\text{--}150\text{ °C}$  (TGA, Fig. S6 in ESI†) or  $40\text{--}170\text{ °C}$  (TGA-IR-MS, Fig. S7†) which corresponds to the removal of the water molecules ( $m/z = 17$  and  $18$  in MS,  $\text{H}_2\text{O}$  bands in IR, TGA obs. 7.6, TGA-IR-MS obs. 9.4%, calcd. 10.4%). The weight loss continues from  $250\text{ °C}$  on without pronounced steps. Between  $250\text{--}326\text{ °C}$   $m/z = 44$  ( $\text{CO}_2$ ) and  $52$  in MS,  $\text{CO}_2$  bands in IR. From  $326\text{ °C}$  on  $m/z = 50, 52, 76, 78, 79, 103, 104, 105$  and  $106$  as typical aromatic fragments (see above and  $105 = [\text{C}_6\text{H}_5\text{-CO}]^+$ ) coming from the  $\text{ip}^{2-}$  moiety (Fig. S8). The TGA-IR shows bands for nitrile,  $\text{HCN}$ ,  $\text{NH}_3$  and/or hydrazine and  $\text{CO}_2$  (Fig. S9 in ESI†). The weight loss continues to  $600\text{ °C}$  where 38.9% (TGA) or 31% (TGA-IR-MS) of the original mass is retained ( $\text{ZnO}$  calcd 23.4%).

**Crystal structure of  $^3\{[\text{Zn}_2(\mu_2\text{-bdc})_2(\mu_4\text{-btre})]\}$ , 1.** The zinc compound **1** features a dinuclear metal unit with two crystallographically different bdc ligands, each of them with an inversion center in the  $\text{C}_6$  centroid. One bdc ligand bridges between two  $\text{Zn}$  atoms with an almost bidentate coordination to each  $\text{Zn}$  while the other bdc ligand bridges between two  $\text{Zn}$  atoms with a monodentate coordination to each metal atom. The btre ligand bridges between four  $\text{Zn}$  atoms and assumes a *cis*-bent geometry (Fig. 1). The central  $\text{C-C}$  bond of the btre ligand is bisected by a  $\text{C}_2$  axis.

The  $\text{Zn}$ -bdc substructure consists of criss-crossed 1D chains (Fig. 2a) while the  $\text{Zn}$ -btre substructure can be pictured as out-of-phase sine-wave chains because of the *cis*-bent btre-ligand geometry (Fig. 2b). Both substructures combine to a densely packed 3D framework (Fig. 3).

**Crystal structure of  $^3\{[\text{Cd}_2(\mu_4\text{-bdc})(\mu_4\text{-btre})_2](\text{NO}_3)_2\cdot\text{H}_2\text{O}\}$ , 2.** The cadmium compound **2** features strands of  $\text{Cd}$  atoms with neighboring  $\text{Cd}$  atoms bridged by two btre-triazole groups and a bdc-carboxylate group. Hence, each  $\text{Cd}$  atom is seven coordinated by four nitrogen and three oxygen atoms. Each  $\text{bdc}^{2-}$  and the *trans*-bent btre ligand bridge between four cadmium atoms (Fig. 4). The bdc carboxylate group coordinates in a chelating-bridging  $\mu\text{-}\kappa\text{O:}\kappa\text{O}'$  mode to the adjacent  $\text{Cd}$  atoms. Thus, one  $\text{O}$  atom of each carboxylate group functions as a bridge between two  $\text{Cd}$  atoms (Fig. 4 and 5a).

The  $\text{Cd}$ -bdc substructure is a 2D layer (Fig. 5a), while the  $\text{Cd}$ -btre substructure is a 3D framework (Fig. 5b). The substructures combine to a 3D framework with channels along  $c$  which are filled

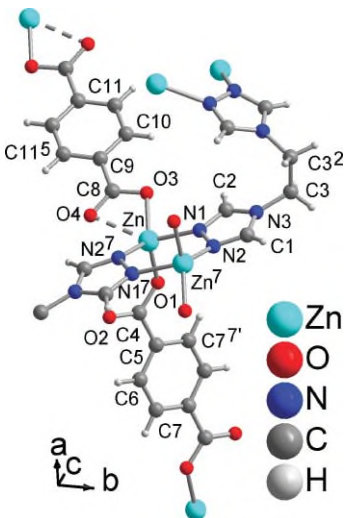


**Fig. 1** Coordination environment for a dinuclear zinc unit in **1**. Selected distances ( $\text{\AA}$ ) and angles ( $^\circ$ ): Zn–O1 1.947(1), Zn–O3 1.961(1), Zn–N2<sup>7</sup> 2.033(1), Zn–N1 2.091(1), Zn–O4 2.471(1), O1–Zn–O3 114.50(4), O1–Zn–N2<sup>7</sup> 109.27(3), O3–Zn–N2<sup>7</sup> 127.62(4), O1–Zn–N1 104.21(3), O3–Zn–N1 93.91(4), N2<sup>7</sup>–Zn–N1 102.01(3), O1–Zn–O4 103.09(3), O3–Zn–O4 58.40(3), N2<sup>7</sup>–Zn–O4 85.24(3), N1–Zn–O4 147.44(3). Symmetry codes in **1**: 2 =  $-1 - x, y, -0.5 - z$ ; 5 =  $-1 - x, -y, -z$ ; 7 =  $-1.5 - x, 0.5 - y, -1 - z$ ; 7' =  $-2.5 - x, 0.5 - y, -1 - z$ .

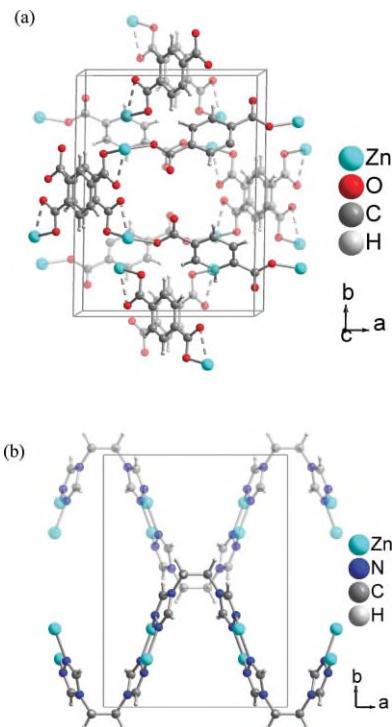


**Fig. 2** Packing analysis for **1** by differentiation in individual (a)  $\{\text{Zn}-\text{btc}\}$ -strands (some semitransparent for clarity) and (b)  $\{\text{Zn}-\text{btre}\}$ -out-of-phase sine-wave chains. The chain in the background in (b) is depicted semitransparent.

by disordered nitrate ions and less than fully occupied crystal water molecules (both of them not shown for clarity in Fig. 6).

**Crystal structure of  $^2\{[\text{Zn}_2(\mu_2-\text{ip})_2(\mu_2-\text{btre})(\text{H}_2\text{O})_2]\cdot 2\text{H}_2\text{O}\}$ , 3.** The zinc compound **3** features a dinuclear metal unit in which

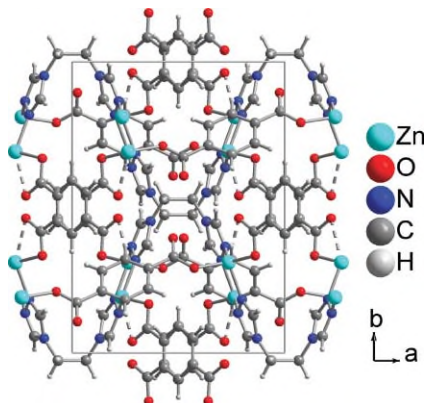


**Fig. 3** Packing diagram for the 3D framework in **1**.

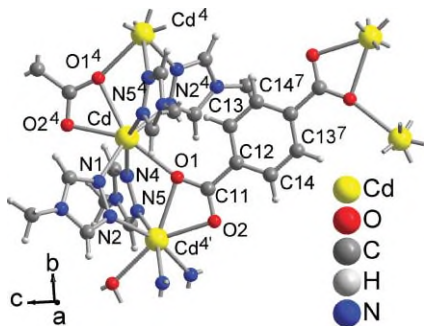


**Fig. 4** Coordination environment in the cadmium strands in **2**. Selected distances ( $\text{\AA}$ ) and angles ( $^\circ$ ): Cd–N4 2.338(3), Cd–N5<sup>4</sup> 2.344(3), Cd–N2<sup>4</sup> 2.345(3), Cd–N1 2.345(3), Cd–O2<sup>4</sup> 2.357(2), Cd–O1 2.427(2), Cd–O1<sup>4</sup> 2.464(2), N4–Cd–N5<sup>4</sup> 159.72(10), N4–Cd–N2<sup>4</sup> 85.13(10), N5<sup>4</sup>–Cd–N2<sup>4</sup> 94.89(10), N4–Cd–N1 90.58(10), N5<sup>4</sup>–Cd–N1 83.66(10), N2<sup>4</sup>–Cd–N1 163.44(10), N4–Cd–O2<sup>4</sup> 83.95(11), N5<sup>4</sup>–Cd–O2<sup>4</sup> 114.44(11), N2<sup>4</sup>–Cd–O2<sup>4</sup> 112.31(11), N1–Cd–O2<sup>4</sup> 83.03(11), N4–Cd–O1 77.70(9), N5<sup>4</sup>–Cd–O1 82.10(9), N2<sup>4</sup>–Cd–O1 84.78(9), N1–Cd–O1 78.68(9), O2<sup>4</sup>–Cd–O1 153.81(9), N4–Cd–O1<sup>4</sup> 121.65(9), N5<sup>4</sup>–Cd–O1<sup>4</sup> 77.97(9), N2<sup>4</sup>–Cd–O1<sup>4</sup> 78.38(9), N1–Cd–O1<sup>4</sup> 117.18(9), O2<sup>4</sup>–Cd–O1<sup>4</sup> 53.58(9), O1–Cd–O1<sup>4</sup> 152.56(7), Cd–O1–Cd<sup>4</sup> 108.14(8). Symmetry codes in **2**: 4 =  $0.5 - x, 0.5 + y, 0.5 - z$ ; 4' =  $0.5 - x, -0.5 + y, 0.5 - z$ ; 7 =  $0.5 - x, 0.5 - y, -z$ .

two inversion symmetry related Zn atoms are bridged by two carboxylate groups. Each Zn atom is coordinated by three carboxyl oxygen atoms, one nitrogen atom from a btre ligand and one aqua ligand to give a five-fold coordination sphere in-between trigonal bipyramidal and square planar ( $\tau = 0.54$ ).<sup>35</sup> Each ip<sup>2-</sup> ligand bridges between three Zn atoms coordinating to each of them monodentate with a different O atom. Each btre ligand connects only two zinc atoms, thereby using only one N atom on each triazolyl ring for metal coordination (different from the other two structures and from the other reported examples).<sup>7,33</sup> The btre ligand assumes a *trans*-bent geometry (Fig. 7).

The Zn-bdc substructure consists of double strands along *b* (Fig. 8a) while the Zn-btre substructure consists of individual Zn-btre-Zn pairs (Fig. 8b).

The btre ligands bridge the Zn-bdc double strands to a 2D double layer (Fig. 9). Neighboring double layers are connected through hydrogen bonds from the aqua ligands.

In compounds **1–3** C–H  $\cdots$  O hydrogen bonds<sup>36,37</sup> are present and in **3**, with its aqua ligand and crystal water, also classical

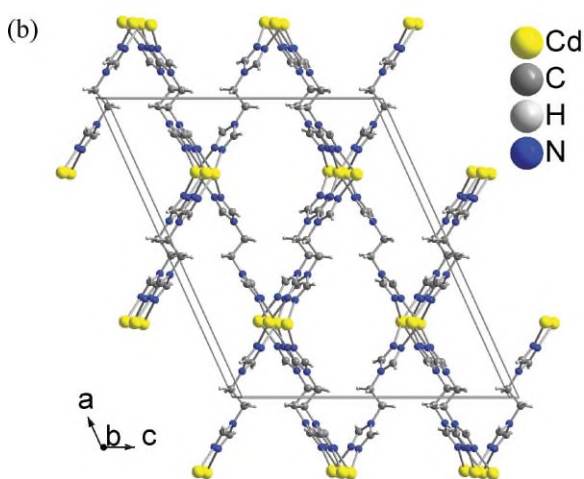
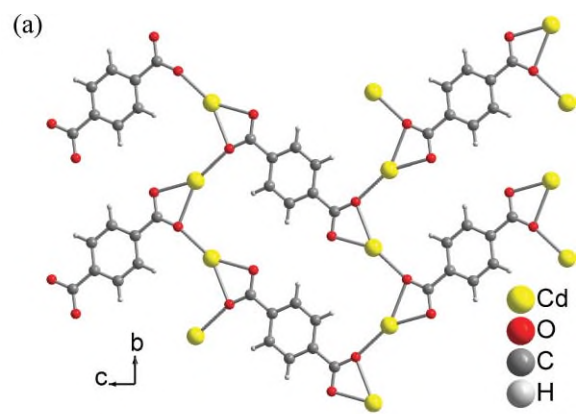


**Fig. 5** Packing analysis for **2** by differentiation in individual (a) {Cd-btc}-nets and (b) {Cd-btre}-frameworks.

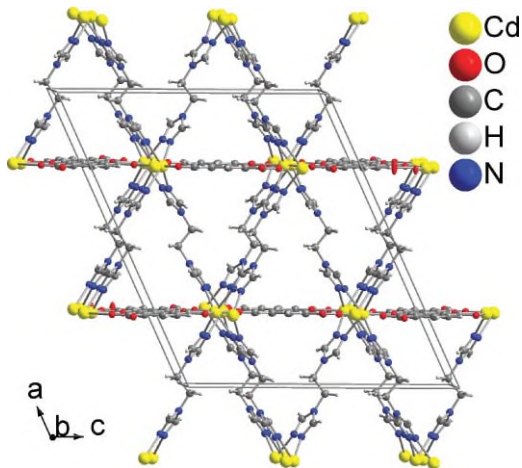


**Fig. 6** Packing diagram for the 3D framework in **2**. Nitrate ions and water molecules in the channels are not shown for clarity.

O–H $\cdots$ O/N hydrogen bonds<sup>38</sup> come into play (see Table S1, Fig. S10–S12 ESI†).

**Solid-state CPMAS NMR of 1–3.** Carbon-13 solid-state NMR should be able to reflect among other things the symmetry of the organic ligand(s) in diamagnetic coordination networks.<sup>39,40</sup> As such, a collection of solid-state NMR spectra for a certain

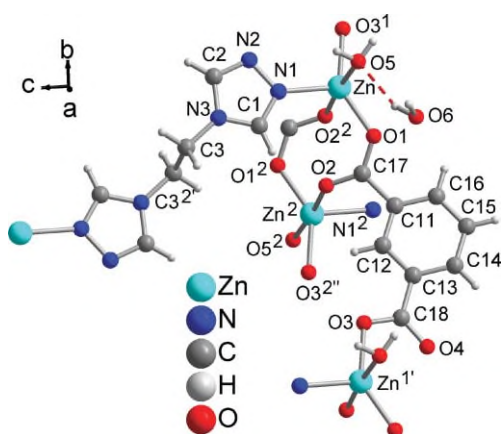


**Fig. 7** Building unit in **3**. Selected distances ( $\text{\AA}$ ) and angles ( $^\circ$ ): Zn–O1 1.981(1), Zn–O3<sup>1</sup> 2.016(1), Zn–N1 2.081(2), Zn–O2<sup>2</sup> 2.145(1), Zn–O5 2.198(2), O1–Zn–O3<sup>1</sup> 142.84(6), O1–Zn–N1 112.75(5), O3<sup>1</sup>–Zn–N1 103.59(5), O1–Zn–O2<sup>2</sup> 90.35(5), O3<sup>1</sup>–Zn–O2<sup>2</sup> 94.99(5), N1–Zn–O2<sup>2</sup> 93.69(5), O1–Zn–O5 85.33(5), O3<sup>1</sup>–Zn–O5 87.59(5), N1–Zn–O5 89.37(6), O2<sup>2</sup>–Zn–O5 175.42(4). Symmetry codes in **3**: 1 =  $-1 + x, 1 + y, z$ ; 1' =  $1 + x, -1 + y, z$ ; 2 =  $-x, 1 - y, 1 - z$ ; 2' =  $-x, 1 - y, 2 - z$ ; 2'' =  $1 - x, -y, 1 - z$ .

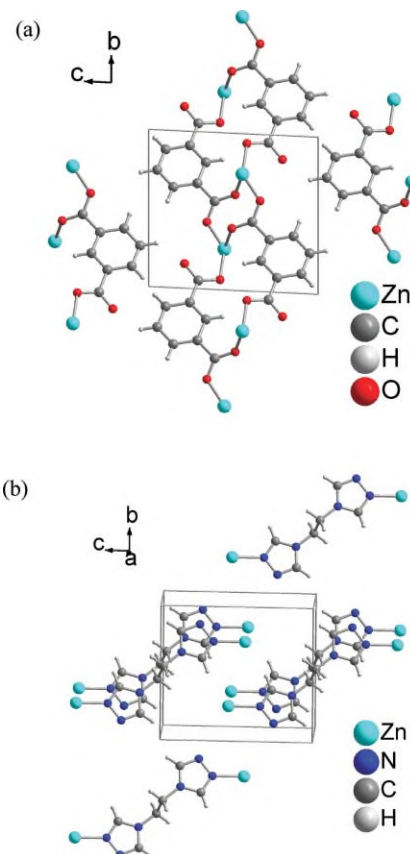


**Fig. 8** Packing analysis for **3** by differentiation in individual (a) {Zn-ip}-double strands and (b) {Zn-btre}-units.

ligand or ligand combination would eventually not only serve as a fingerprint but as a tool to predict the network topology, the nature and stereochemistry of hitherto structurally uncharacterized solid, amorphous or poorly crystalline coordination polymers.<sup>41</sup> Also, solid-state NMR can be a structurally informative

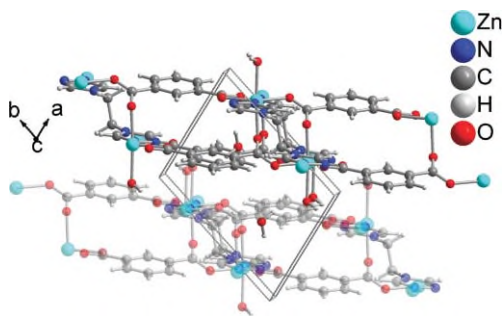


**Fig. 9** Packing diagram of **3** showing two double layers with one of them semitransparent for clarity. The water molecules of crystallization in the channels are not shown for clarity.

technique for materials containing stoichiometric paramagnetic Cu(I)/Cu(II)/Zn(II) constituents.<sup>42</sup> Structural studies in the solid state by <sup>13</sup>C and <sup>15</sup>N CPMAS NMR spectroscopy carried out on a series of 2-aminotroponeimine derivatives have allowed to establish the existence of hydrogen bonding and to determine the most stable tautomer.<sup>43</sup> So far, we are not aware of many in-depth solid-state NMR investigations of coordination networks.

The <sup>13</sup>C CPMAS spectrum of **1** in Fig. 10 shows 9 out of 11 signals expected for the symmetry-different (unique) carbon atoms. From the peak integrals the bdc:btre ligand ratio is 2:1.

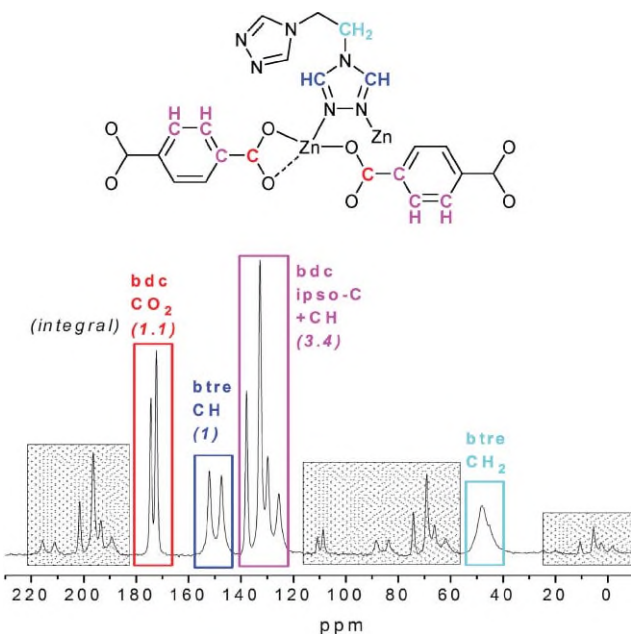


**Fig. 10** <sup>13</sup>C CPMAS NMR spectrum for **1** and schematic drawing of the building unit with the unique ligand parts given in bold atom symbols. Integral of btre CH set to 1. Regions with rotation side bands at 8 (16) kHz = 64 (128) ppm from the signal are covered in the NMR spectrum. Peak positions: 174.4, 173.3, 152.0, 147.4, 137.9, 132.8, 129.3, 125.6 and 48.1 ppm.

The <sup>13</sup>C CPMAS spectrum of **2** in Fig. 11 shows 3 out of 4 signals expected for the 2 unique CH, the ipso- and  $\text{CO}_2$  atom of the bdc ligand. For the two symmetry independent triazol rings only one, slightly broadened CH peak is observed for the four crystallographically different btre CH positions. This peak consists of more than one resonance which could not be resolved. This may

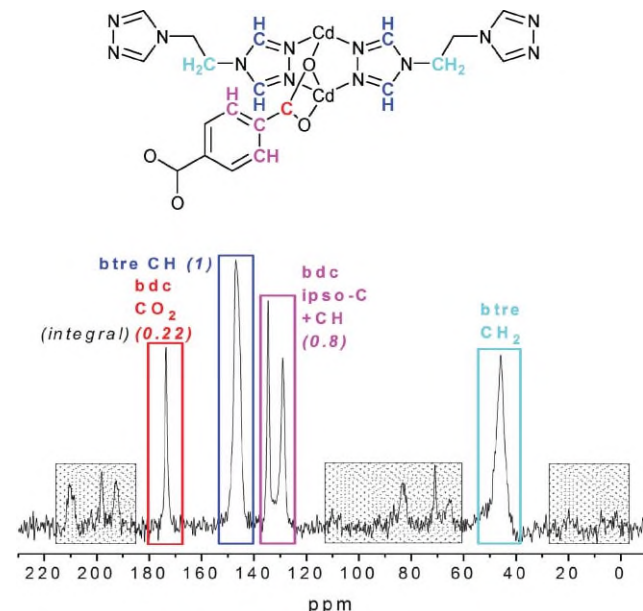


**Fig. 11** <sup>13</sup>C CPMAS NMR spectrum for **2** and schematic drawing of the building unit with the unique ligand parts given with bold atom symbols. Integral of btre CH set to 1. Regions with rotation side bands at 8 (16) kHz = 64 (128) ppm from the signal are covered in the NMR spectrum. Peak positions: 172.6, 147.0, 134.5, 129.0 and 45.9 ppm.

also be due to a symmetry (space group) change with temperature as the NMR is measured at ambient temperature ( $\sim 30^\circ\text{C}$ ), while the X-ray data set is collected at low temperature ( $-70^\circ\text{C}$ ). The peak integrals agree with the bdc:btre ligand ratio of 1:2.

A closer inspection of the crystal structure of **2** reveals a pseudo mirror plane formed by the Cd atoms in the strand and also by the Cd-bdc layer (Fig. 12, cf. Fig. 6). Such a mirror plane would render the two triazol rings symmetry equivalent. Furthermore, the environment for the two CH atoms in each triazol ring is very similar (Fig. 12). Together this explains the near-equivalency of the btre CH atoms leading to a broadening but no splitting of the peak.

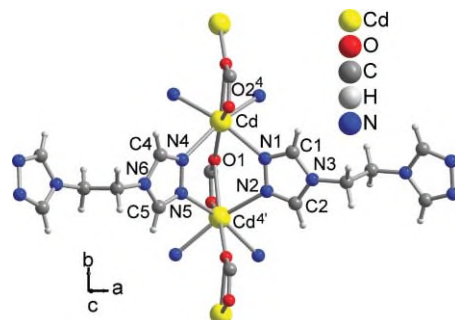


**Fig. 12** View along the pseudo mirror plane through the Cd atoms and the Cd-bdc layer in **2** (cf. Fig. 6) to illustrate the near-equivalency of the two triazol rings with C1,C2 and C4,C5.

The <sup>13</sup>C CPMAS spectrum of **3** in Fig. 13 is similar to the spectrum of **1** in Fig. 10 and shows 9 out of 11 signals expected for the symmetry-different (unique) carbon atoms of the ligands. Also, the peak integral of the benzene-dicarboxylate (ip) and btre

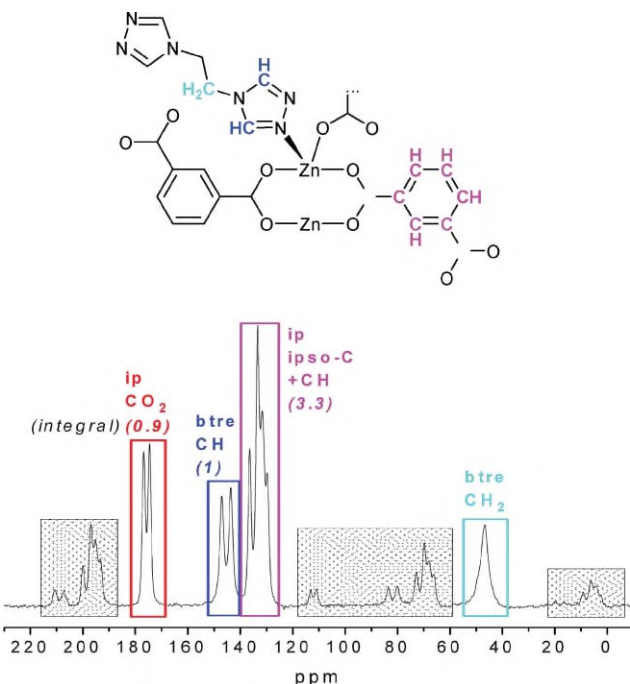


**Fig. 13**  $^{13}\text{C}$  CPMAS NMR spectrum for **3** and schematic drawing of the building unit with the unique ligand parts given with bold atom symbols. Integral of btre CH set to 1. Regions with rotation side bands at 8 (16) kHz = 64 (128) ppm from the signal are covered in the NMR spectrum. Peak positions: 176.7, 174.6, 147.1, 143.7, 136.3, 133.3, 131.5, 129.7 and 46.7 ppm.

signals is as seen in **1** (Fig. 10) and agrees with the ip:btre ligand ratio of 2:1.

**Luminescence properties of **1–3**.** The  $d^{10}$  zinc and cadmium mixed-bdc/ip-btre-ligand coordination polymers **1–3** show strong fluorescence emissions at 445 (**1**), 421 (**2**) and 423 nm (**3**) upon excitation at 335 (**1**), 328 (**2**) and 320 nm (**3**) (Fig. 14). The free 1,2-bis(1,2,4-triazol-4-yl)ethane ligand (btre) gives no fluorescence response at room temperature. A possible btre fluorescence through an intra-ligand charge transfer is apparently quenched by the thermal intra-ligand rotations around the C–C and C–N bonds.

## Conclusions

The ligand combination of 1,2-bis(1,2,4-triazol-4-yl)ethane (btre) and fully deprotonated benzene-1,3- or -1,4-dicarboxylate (ip<sup>2-</sup> or bdc<sup>2-</sup>) with zinc and cadmium cations leads to 3D (with bdc<sup>2-</sup>) or 2D (with ip<sup>2-</sup>) metal–organic frameworks. The bdc/ip to btre ligand ratio and the ligand local site symmetry is reflected in the solid-state CPMAS  $^{13}\text{C}$  NMR spectra. Zinc or cadmium coordination to benzenedicarboxylate and the btre ligand gives a strong luminescence response upon UV excitation (the free btre ligand is non-luminescent). Further studies on the luminescent properties of metal-btre compounds are in progress.

## Experimental

Commercially available solvents, monoformylhydrazine, triethyl orthoformate, ethylenediamine, benzene-1,4-dicarboxylic acid

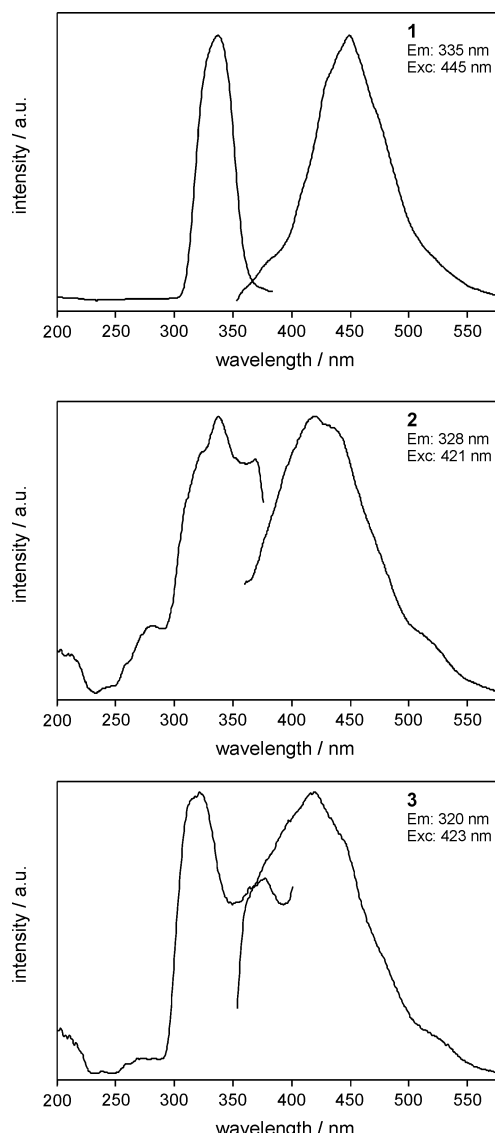


**Fig. 14** Excitation (Exc) and emission (Em) spectra of compounds **1–3**; the respective excitation (emission spectra) and monitoring (excitation spectra) wavelengths are given.

(H<sub>2</sub>bdc), benzene-1,3-dicarboxylic acid (H<sub>2</sub>ip), triethylamine, Zn(NO<sub>3</sub>)<sub>2</sub>·4H<sub>2</sub>O and Cd(NO<sub>3</sub>)<sub>2</sub>·4H<sub>2</sub>O were used without further purification. The ligand 1,2-bis(1,2,4-triazol-4-yl)ethane (btre) was prepared according to the method from Bayer.<sup>44</sup> Dried methanol is used for the preparation of the btre ligand. Elemental analyses were performed on a VarioEL from Elementaranalysensysteme GmbH. Infrared spectra were recorded in the range 400–4000 cm<sup>-1</sup> on a Bruker Optik IFS 25 spectrophotometer using KBr pellets. Thermogravimetric analysis was carried out in a simultaneous thermoanalysis apparatus STA 409C from Netzsch under nitrogen with a heating rate of 10 °C min<sup>-1</sup> in the range 50 to 600 °C. The filled sample container was conditioned by first applying oil pump vacuum down to 1 bar for 5 min, then flushing with nitrogen. TGA-IR and TGA-MS were recorded simultaneously on the Mettler TGA/SDTA 851e coupled with the Nicolet Nexus 470 gas phase FTIR and the Balzers (Pfeiffer Vacuum) Quadrupole MS. Experiments were done under Argon

(60 ml/min) in 900  $\mu$ L alox crucibles between 30 and 600°C with 10°C/min. Powder X-ray diffraction patterns were measured at ambient temperature using a STOE STADI-P with Debye-Scherrer geometry, Mo-K $\alpha$  radiation ( $\lambda = 0.7093 \text{ \AA}$ ), a Ge(111) monochromator and the samples in glass capillaries on a rotating probe head. Simulated powder patterns were based on single-crystal data and calculated using the STOE WinXPOW software package.<sup>45</sup>

## Syntheses

**catena-[ $(\mu_2\text{-Benzene-1,4-dicarboxylato-\kappa}^2O,\text{O':\kappa}^2O'',\text{O'''})(\mu_2\text{-benzene-1,4-dicarboxylato-\kappa}O:\text{k}O')-(\mu_4\text{-1,2-bis(1,2,4-triazol-4-yl)ethane-\kappa}N1:\text{k}N1':\text{k}N2:\text{k}N2')$ -dizinc(II)],  $^3\{\text{[Zn}_2(\mu_2\text{-bdc})_2(\mu_4\text{-btre})]\}$  (1).** A mixture of Zn(NO<sub>3</sub>)<sub>2</sub>·4H<sub>2</sub>O (131 mg, 0.50 mmol), H<sub>2</sub>bdc (83 mg, 0.50 mmol), btre (82 mg, 0.50 mmol) and water (15 mL) was stirred for 30 min. at room temperature and the pH value of the final mixture was adjusted to 6.50 by addition of triethylamine, then the mixture is transferred to a Teflon-lined stainless-steel autoclave and heated at 160 °C for 3 d, then it was cooled to room temperature at a rate of 10 °C h<sup>-1</sup>. A colorless crystalline product, which was suitable for X-ray single crystal analysis, was filtered off, washed with distilled water and dried in air (Yield 96 mg, 62% based on Zn). Elemental analysis C<sub>22</sub>H<sub>16</sub>Zn<sub>2</sub>N<sub>6</sub>O<sub>8</sub> (623.18) calcd. C 42.40, H 2.59, N 13.49; found: C 42.80, H 2.74, N 13.06%; IR (KBr) 3102(w), 3050(w), 3008(w), 1602(s, v<sub>asym</sub>CO<sub>2</sub>), 1570(m, v<sub>asym</sub>CO<sub>2</sub>), 1503(m), 1445(m, v<sub>sym</sub>CO<sub>2</sub>), 1395(m, v<sub>sym</sub>CO<sub>2</sub>), 1342(m), 1204(m), 1169(m), 1141(m), 1078(s), 1046(s), 1013(s), 940(w), 915(w), 888(m), 842(s), 812(s), 750(s), 648(s), 586(s), 514(m), 471(w) cm<sup>-1</sup>.

**catena-[ $(\mu_4\text{-Benzene-1,4-dicarboxylato-\kappa}O:\text{k}^2O,\text{O':\kappa}^2O'',\text{O'''}\text{-bis}(\mu_4\text{-1,2-bis(1,2,4-triazol-4-yl)ethane-\kappa}N1:\text{k}N1':\text{k}N2:\text{k}N2')$ -dicadmium(II) dinitrate hydrate,  $^3\{\text{[Cd}_2(\mu_4\text{-bdc})(\mu_4\text{-btre})]_2(\text{NO}_3)_2\cdot\text{H}_2\text{O}\}$  (2).** A mixture of Cd(NO<sub>3</sub>)<sub>2</sub>·4H<sub>2</sub>O (154 mg, 0.50 mmol), H<sub>2</sub>bdc (83mg, 0.50 mmol), btre (82 mg, 0.50 mmol) and water (15 mL) was stirred for 30 min. at room temperature and the pH value of the final mixture was adjusted to 5.00 by addition of triethylamine, then the mixture is transferred to a Teflon-lined stainless-steel autoclave and heated at 160 °C for 3 d, then it was cooled to room temperature at a rate of 10 °C h<sup>-1</sup>. A colorless crystalline product, which was suitable for X-ray single crystal analysis, was filtered off, washed with distilled water and dried in air (Yield 115 mg, 54% based on Cd). Elemental analysis C<sub>20</sub>H<sub>22</sub>Cd<sub>2</sub>N<sub>14</sub>O<sub>11</sub> (859.32) calcd. C 27.96, H 2.58, N 22.82; found: C 27.61, H 2.26, N 22.67%; IR (KBr) 3442(w, v(O-H)), 3110(w), 1656(m, v<sub>asym</sub>CO<sub>2</sub>), 1553(s, v<sub>asym</sub>CO<sub>2</sub>), 1504(s), 1434(m, v<sub>sym</sub>CO<sub>2</sub>), 1378(s, v<sub>sym</sub>CO<sub>2</sub>), 1342(w), 1286(w), 1202(s), 1160(m), 1112(w), 1079(s), 1032(m), 1016(m), 993(m), 884(m), 844(s), 746(s), 684(m), 640(s), 526(s), 488(w) 457(w), 407(w) cm<sup>-1</sup>.

**catena-[Diaqua-bis( $\mu_3\text{-benzene-1,3-dicarboxylato-\kappa}O:\text{k}O'\text{-}\mu_2\text{-1,2-bis(1,2,4-triazol-4-yl)ethane-\kappa}N1:\text{k}N1')$ -dizinc(II)] dihydrate,  $^2\{\text{[Zn}_2(\mu_3\text{-ip})_2(\mu_2\text{-btre})(\text{H}_2\text{O})_2\}\cdot2\text{H}_2\text{O}\}$  (3).** A mixture of Zn(NO<sub>3</sub>)<sub>2</sub>·4H<sub>2</sub>O (131 mg, 0.50 mmol), H<sub>2</sub>ip (83mg, 0.50 mmol), triethylamine (140  $\mu$ L, 1.50 mmol), btre (82 mg, 0.50 mmol) and water (15 mL) was stirred for 30 min. at room temperature, then the mixture is transferred to a Teflon-lined stainless-steel autoclave and heated at 180 °C for 3 d, then it was cooled to room temperature at a rate of 2.8 °C h<sup>-1</sup>. A colorless crystalline

product, which was suitable for X-ray single crystal analysis was filtered off, washed with distilled water and dried in air (Yield 120 mg, 69% based on Zn). Elemental analysis C<sub>22</sub>H<sub>24</sub>Zn<sub>2</sub>N<sub>6</sub>O<sub>12</sub> (695.26) calcd. C 38.01, H 3.48, N 12.09; found: C 38.02, H 3.75, N 12.32%; IR (KBr) 3566 and 3497(w, v(O-H)), 3122(w), 1609(s, v<sub>asym</sub>CO<sub>2</sub>), 1562(s, v<sub>asym</sub>CO<sub>2</sub>), 1479(m), 1429(s, v<sub>sym</sub>CO<sub>2</sub>), 1371(s, v<sub>sym</sub>CO<sub>2</sub>), 1273(w), 1195(m,  $\delta(\text{OH}\cdots\text{O})$ ), 1174(w), 1078(m), 1018(m), 981(w), 900(m,  $\gamma(\text{OH}\cdots\text{O})$ ), 824(m), 800(w), 752(s), 720(s), 686(m), 640(s), 576(m), 463(w), 434(w), 408(w) cm<sup>-1</sup>.

## X-Ray crystallography†

Suitable single crystals were carefully selected under a polarizing microscope. *Data collection:* Bruker AXS with APEX2 CCD area-detector, temperature 203(2) K, Mo-K $\alpha$  radiation ( $\lambda = 0.71073 \text{ \AA}$ ), graphite monochromator, double-pass method  $\omega$ -scan. Data collection with APEX2, cell refinement and data reduction with SAINT,<sup>46</sup> experimental absorption correction with SADABS.<sup>47</sup> *Structure analysis and refinement:* The structure was solved by direct methods (SHELXS-97); refinement was done by full-matrix least squares on  $F^2$  using the SHELXL-97 program suite.<sup>48</sup> All non-hydrogen positions refined with anisotropic displacement parameters. Hydrogen atoms were positioned geometrically (aromatic C-H = 0.94 Å, 0.98 Å for CH<sub>2</sub>) and refined using a riding model (AFIX 43 for aromatic CH, AFIX 23 for CH<sub>2</sub>) with U<sub>iso</sub>(H) = 1.2 U<sub>eq</sub>(CH, CH<sub>2</sub>). In **2** the nitrate ions are disordered over at least two positions. Their N and O atoms could only be refined isotropically. The crystal water molecule in **2** is disordered over two positions with about 0.25 occupancy, each. Only the oxygen atoms could be found and refined isotropically. In **3** hydrogen atoms on the aqua ligands and the crystal water were found and refined with U<sub>iso</sub>(H) = 1.5U<sub>eq</sub>(O). Simulated X-ray powder diffractograms from the single-crystal data were matched with measured X-ray powder diffractograms for **1**, **2** and **3** to verify the representative nature of the single crystal with respect to the bulk material (Fig. S1-S3 ESI).† Graphics were obtained with DIAMOND.<sup>49</sup> Crystal data and details on the structure refinement are given in Table 1.

## Luminescence measurements

Photoluminescence analyses for compounds **1**, **2** and **3** were performed using powdered samples at room temperature in diffuse reflection geometry on a Perkin Elmer LS55 fluorescence spectrometer equipped with a Xe discharge lamp (equivalent to 20 kW for 8  $\mu$ s duration) and a gated photomultiplier with modified S5 response. The acquisition time was 100 nm/min.

## CPMAS NMR

All spectra were recorded using 2.5 mm rotors on a Bruker Avance 500 solid-state NMR spectrometer (11.7 T) operating at Larmor frequencies of 125.78 MMz for <sup>13</sup>C. RF pulses were applied at a transverse B1 field of 125 kHz corresponding to a  $\pi/2$  pulse width of 2  $\mu$ s. <sup>13</sup>C {<sup>1</sup>H} CPMAS experiments were performed under magic angle spinning at 8 KHz with bearing gas at ambient temperature. Cross polarization was achieved using a ramp<sup>50</sup> with typically 1024 steps applied to the proton channel ranging from 80 to 100% and a contact time of 2 ms. In all <sup>13</sup>C experiments, TPPM

**Table 1** Crystal data and structure refinement for **1** to **3**

Compound	<b>1</b>	<b>2</b>	<b>3</b>
Empirical formula	$C_{11}H_8ZnN_3O_4^e$	$C_{10}H_{11}CdN_7O_{5.5}^{ef}$	$C_{11}H_{12}ZnN_3O_6^e$
M/g mol <sup>-1</sup>	311.59 <sup>e</sup>	429.66 <sup>ef</sup>	347.63 <sup>e</sup>
Crystal size/mm	0.60 × 0.25 × 0.20	0.32 × 0.12 × 0.02	0.25 × 0.09 × 0.01
2θ range/ <sup>o</sup>	4.6–77.2	3.9–51.7	6.1–71.0
Completeness to 20%/	100 <sup>g</sup>	99.8	96.8 <sup>g</sup>
h; k; l range	±22; -26, +25; -22, +23	±28; ±9; ±23	-12, +9; -15, +9; -13, +16
Crystal system	Monoclinic	Monoclinic	Triclinic
Space group	C2/c	C2/c	P-1
a/Å	12.455(1)	22.9206(8)	7.4247(2)
b/Å	15.158(1)	7.7047(2)	9.3631(2)
c/Å	13.274(2)	19.3208(7)	10.1580(2)
α/°	90.00	90	81.657(1)
β/°	117.43(1)	114.596(3)	70.675(1)
γ/°	90.00	90	71.704(1)
V/Å <sup>3</sup>	2224.3(4)	3102.4(2)	632.02(3)
Z	8	8	2
D <sub>calc</sub> /g cm <sup>-3</sup>	1.861	1.840 <sup>f</sup>	1.827
F (000)	1256	1696 <sup>f</sup>	354
μ/mm <sup>-1</sup>	2.223	1.449 <sup>f</sup>	1.977
Max/min transmiss.	0.6382/0.3349	0.9716/0.6543	0.9805/0.6378
Refl. collected ( $R_{int}$ )	46785 (0.0288)	20459 (0.0395)	8293 (0.0192)
Indep. reflections	6281	3001	4087
Obs. refl. [ $I > 2\sigma(I)$ ]	5188	2633	3464
Parameters refined	172	216	202
Max./min. Δρ/e Å <sup>-3a</sup>	0.614/-0.294	1.581/-0.589	0.472/-0.335
$R_1/wR_2$ ; [ $I > 2\sigma(I)$ ] <sup>b</sup>	0.0263/0.0676	0.0285/0.0745	0.0304/0.0702
$R_1/wR_2$ (all reflect.) <sup>b</sup>	0.0376/0.0719	0.0334/0.0774	0.0394/0.0741
Goodness-of-fit on $F^2$ <sup>c</sup>	1.024	1.053	1.038
Weight. scheme w; a/b <sup>d</sup>	0.0397/0.7942	0.0438/10.1578	0.0350/0.2008

<sup>a</sup> Largest difference peak and hole. <sup>b</sup>  $R_1 = [\sum(|F_o| - |F_c|)/\sum|F_o|]; wR_2 = [\sum[w(F_o^2 - F_c^2)^2]/\sum[w(F_o^2)^2]]^{1/2}$ . <sup>c</sup> Goodness-of-fit =  $[\sum[w(F_o^2 - F_c^2)^2]/(n - p)]^{1/2}$ . <sup>d</sup>  $w = 1/[\sigma^2(F_o^2) + (aP)^2 + bP]$  where  $P = (\max(F_o^2 \text{ or } 0) + 2F_c^2)/3$ . <sup>e</sup> Throughout the text the doubled formula of the asymmetric unit was used to have full ligand numbers. <sup>f</sup> H atoms on crystal water not located but included in formula, formula mass, density, F (000) and μ calculation. <sup>g</sup> Completeness to 2θ = 50°.

dipolar decoupling<sup>51</sup> was employed. <sup>13</sup>C spectra were referenced to the methyne resonance of alanine (51 ppm).

## Acknowledgements

The work is supported by KAAD and DFG grant Ja466/14-1. We thank Dr Pierre Fux and the Research Analytics Department of Ciba Inc., Basel, Switzerland for the TG-IR-MS experiments.

## Notes and references

- Reviews about coordination polymers/MOFs: *Application oriented properties*: C. Janiak, *Dalton Trans.*, 2003, 2781–2804; S. L. James, *Chem. Soc. Rev.*, 2003, **32**, 276–288; U. Mueller, M. Schubert, F. Teich, H. Puetter, K. Schierle-Arndt and J. Pastré, *J. Mater. Chem.*, 2006, **16**, 626–636; N. R. Champness, *Dalton Trans.*, 2006, 877–880; X. Lin, J. Jia, P. Hubberstey, M. Schröder and N. R. Champness, *CrystEngComm*, 2007, **9**, 438–448; C. Janiak, *Angew. Chem. Int. Ed.*, 1997, **36**, 1431–1434; *4,4'-Bipyridine-ligands*: K. Biradha, M. Sarkar and L. Rajput, *Chem. Commun.*, 2006, 4169–4179; *2,2'-Bipyridine- and carboxylate-ligands*: B.-H. Ye, M.-L. Tong and X.-M. Chen, *Coord. Chem. Rev.*, 2005, **249**, 545–565; *Chirality*: B. Kesani and W. Lin, *Coord. Chem. Rev.*, 2003, **246**, 305–326; *f-Elements*: C. L. Cahill, D. T. de Lill and M. Frisch, *CrystEngComm*, 2007, **9**, 15–26; Y. Zhou, M. Hong and X. Wu, *Chem. Commun.*, 2006, 135–143; *Silver(I)*: C.-L. Chen, B.-S. Kang and C.-Y. Su, *Aust. J. Chem.*, 2006, **59**, 3–18; *Imidazolate-, triazolate-ligands*: J.-P. Zhang and X.-M. Chen, *Chem. Commun.*, 2006, 1689–1699; *Interpenetration*: V. A. Blatov, L. Carlucci, G. Ciani and D. M. Proserpio, *CrystEngComm*, 2004, **6**, 377–395; L. Carlucci, G. Ciani and D. Proserpio, *Coord. Chem. Rev.*, 2003, **246**, 247–289; *Magnetism*:

D. MasPOCH, D. Ruiz-Molina and J. Veciana, *Chem. Soc. Rev.*, 2007, **36**, 770–818; D. MasPOCH, D. Ruiz-Molina and J. Veciana, *J. Mater. Chem.*, 2004, **14**, 2713–2723; S. R. Batten and K. S. Murray, *Coord. Chem. Rev.*, 2003, **246**, 103–130; *O- and N-donors*: A. Y. Robin and K. M. Fromm, *Coord. Chem. Rev.*, 2006, **250**, 2127–2157; Porosity: G. Férey, *Chem. Soc. Rev.*, 2008, **37**, 191–214; S. Kitagawa and R. Matsuda, *Coord. Chem. Rev.*, 2007, **251**, 2490–2509; S. Kitagawa, S.-I. Noro and T. Nakamura, *Chem. Commun.*, 2006, 701–707; C. J. Kepert, *Chem. Commun.*, 2006, 695–700; S. Kitagawa and K. Uemura, *Chem. Soc. Rev.*, 2005, **34**, 109–119.

- Recent examples on luminescence in coordination polymers/metal-organic frameworks: C. Daiguebonne, N. Kerbellec, O. Guillou, J.-C. Bünzli, F. Gumy, L. Catala, T. Mallah, N. Audebrand, Y. Gérault, K. Bernot and G. Calvez, *Inorg. Chem.*, 2008, **47**, 3700–3708; E. Chelebaeva, J. Larionova, Y. Guari, R. A. Sa Ferreira, L. D. Carlos, F. A. Almeida Paz, A. Trifonov and C. Guerin, *Inorg. Chem.*, 2008, **47**, 775–777; P. Zhang, Y.-Y. Niu, B. L. Wu, H.-Y. Zhang, C.-Y. Niu and H.-W. Hou, *Inorg. Chim. Acta*, 2008, **361**, 2609–2615; J.-W. Ye, J. Wang, J.-Y. Zhang, P. Zhang and Y. Wang, *CrystEngComm*, 2007, **9**, 515–523; Q. Chu, L.-Y. Kong, T. Okamura, H. Kawaguchi, W.-L. Meng, W.-Y. Sun and N. Ueyama, *Z. Anorg. Allg. Chem.*, 2007, **633**, 326–331; P. I. Girginova, F. A. A. Paz, P. C. R. Soares-Santos, R. A. S. Ferreira, L. D. Carlos, V. S. Amaral, J. Klinowski, H. I. S. Nogueira and T. Trindade, *Eur. J. Inorg. Chem.*, 2007, 4238–4246.

- Recent examples on magnetism in coordination polymers/metal-organic frameworks: H. A. Habib, J. Sanchiz and C. Janiak, *Dalton Trans.*, 2008, 4877–4884; K. Drabent, Z. Ciunik and A. Ozarowski, *Inorg. Chem.*, 2008, **47**, 3358–3365; D. G. Branzea, L. Sorace, C. Maxim, M. Andruh and A. Caneschi, *Inorg. Chem.*, 2008, **47**, 6590–6592; R. Sessoli, *Inorg. Chim. Acta*, 2008, **361**, 3356–3364; E. Rentschler and C. von Malotki, *Inorg. Chim. Acta*, 2008, **361**, 3646–3653; G. S. Matouzenko, M. Perrin, B. Le Guennic, C. Genet, G. Molnar, A. Bousseksou and S. A. Borshch, *Dalton Trans.*, 2007, 934–942;

- K. Abu-Shandi, H. Winkler and C. Janiak, *Z. Anorg. Allg. Chem.*, 2006, **632**, 629–633; K. Abu-Shandi and C. Janiak, *Z. Naturforsch.*, 2005, **60b**, 1250–1254; J. Chakraborty, M. Nandi Mahasweta, H. Mayer-Figge, W. S. Sheldrick, L. Sorace, A. Bhaumik and P. Banerjee, *Eur. J. Inorg. Chem.*, 2007, 5033–5044; M. Seredyuk, A. B. Gaspar, M. C. Munoz, M. Verdaguera, F. Villain and P. Guetlich, *Eur. J. Inorg. Chem.*, 2007, 4481–4491.
- 4 Recent examples on structural work in coordination polymers/metal-organic framework: D. Jia, A. Zhu, J. Deng, Y. Zhang and J. Dai, *Dalton Trans.*, 2007, 2083–2086; N. Sato and S.-I. Nishikiori, *Dalton Trans.*, 2007, 1115–1119; J. E. Beves, E. C. Constable, C. E. Housecroft, C. J. Kepert and D. J. Price, *CrystEngComm*, 2007, **9**, 456–459; P. Thuéry, *CrystEngComm*, 2007, **9**, 460–462; X. Gu and D. Xue, *CrystEngComm*, 2007, **9**, 471–477; S. M. Krishnan, N. M. Patel, W. R. Knapp, R. M. Supkowski and R. L. LaDuc, *CrystEngComm*, 2007, **9**, 503–514; R. Carballo, B. Covelo, E. García-Martínez, A. B. Lago and E. M. Vázquez-López, *Z. Anorg. Allg. Chem.*, 2007, **633**, 780–782; K. Mueller-Buschbaum and Y. Mokaddem, *Z. Anorg. Allg. Chem.*, 2007, **633**, 521–523; W. R. Knapp, J. G. Thomas, D. P. Martin, M. A. Braverman, R. J. Trovitch and R. L. LaDuc, *Z. Anorg. Allg. Chem.*, 2007, **633**, 575–581; A. Roth, A. Buchholz and W. Plass, *Z. Anorg. Allg. Chem.*, 2007, **633**, 383–392; K. Abu-Shandi, H. Winkler, H. Paulsen and R. Glaum, *Z. Anorg. Allg. Chem.*, 2005, **631**, 2705–2714; Biao Wu, C. Janiak, S.-H. Cho, T. Gadzikwa, M. Afshari, S. T. Nguyen and J. Hupp, *Eur. J. Inorg. Chem.*, 2007, 4863–4867; C. He, Y. Zhao, D. Guo, Z. Lin and C. Duan, *Eur. J. Inorg. Chem.*, 2007, 3451–3463.
- 5 Review: S.-L. Zheng and X.-M. Chen, *Aust. J. Chem.*, 2004, **57**, 703–712.
- 6 U. H. F. Bunz, *Chem. Rev.*, 2000, **100**, 1605; D. M. Ciurtin, N. G. Pschirer, M. D. Smith, U. H. F. Bunz and H. C. zur Loye, *Chem. Mater.*, 2001, **13**, 2743; C. Seward, W. L. Jia, R. Y. Wang, G. D. Enright and S. N. Wang, *Angew. Chem. Int. Ed.*, 2004, **43**, 2933; S. Z. Wu, F. Zeng, H. P. Zhu and Z. Tong, *J. Am. Chem. Soc.*, 2005, **127**, 2048.
- 7 H. A. Habib, J. Sanchiz and C. Janiak, *Dalton Trans.*, 2008, 1734–1744.
- 8 Recent examples for mixed-ligand coordination polymers: B. Wisser Yirong Lu and C. Janiak, *Z. Anorg. Allg. Chem.*, 2007, **633**, 1189–1192; S. C. Manna, K.-I. Okamoto, E. Zangrandi and N. R. Chaudhuri, *CrystEngComm*, 2007, **9**, 199–292; Z.-F. Chen, S.-F. Zhang, H.-S. Luo, B. F. Abrahams and H. Liang, *CrystEngComm*, 2007, **9**, 27–29; A. Pichon, C. M. Fierro, M. Nieuwenhuizen and S. James, *CrystEngComm*, 2007, **9**, 449–451; J. Pasán, J. Sanchiz, F. Lloret, M. Julve and C. Ruiz-Pérez, *CrystEngComm*, 2007, **9**, 478–487; M. D. Stephenson and M. J. Hardie, *Dalton Trans.*, 2006, 3407–3417; R. Carballo, B. Covelo, E. M. Vázquez-López, E. García-Martínez, A. Castañeras and C. Janiak, *Z. Anorg. Allg. Chem.*, 2005, **631**, 2006–2010.
- 9 J.-P. Zhang and X.-M. Chen, *Chem. Commun.*, 2006, 1689–1699; A. Rodriguez-Dieguez, A. Salinas-Castillo, S. Galli, N. Masciocchi, J. M. Gutierrez-Zorrilla, P. Vitoria and E. Colacio, *Dalton Trans.*, 2007, 1821–1828.
- 10 B. Paul, B. Zimmermann, K. M. Fromm and C. Janiak, *Z. Anorg. Allg. Chem.*, 2004, **630**, 1650–1654.
- 11 A. Carton, A. Mesbah, L. Perrin and M. Francois, *Acta Cryst.*, 2007, **E63**, m948–m958; S. C. Manna, E. Zangrandi, J. Ribas and N. R. Chaudhuri, *Dalton Trans.*, 2007, 1383–1391; S. Banerjee, P.-G. Lassahn, C. Janiak and A. Ghosh, *Polyhedron*, 2005, **24**, 2963–2971.
- 12 H. X. Zhang, B.-S. Kang, A.-W. Xu, Z.-N. Chen, Z.-Y. Zhou, A. S. C. Chan, K.-B. Yu and C. Ren, *J. Chem. Soc. Dalton Trans.*, 2001, 2559.
- 13 K.-Y. Choi, K.-M. Chun, K.-C. Lee and J. Kim, *Polyhedron*, 2002, **21**, 1913.
- 14 B.-L. Chen, K.-F. Mok, S.-C. Ng and M. G. B. Drew, *New J. Chem.*, 1999, **23**, 877.
- 15 C. S. Hong and Y. Do, *Inorg. Chem.*, 1997, **36**, 5684.
- 16 H. K. Fun, S. S. S. Raj, R. G. Xiong, J. L. Zuo, Z. Yu and X. Z. You, *J. Chem. Soc. Dalton Trans.*, 1999, 1915.
- 17 J. Cano, G. D. Munno, J. L. Sanz, R. Ruiz, J. Faus, F. Lloret, M. Julve and A. Caneschi, *J. Chem. Soc. Dalton Trans.*, 1997, 1915, and references therein.
- 18 S. A. Bourne, J. Lu, A. Mondal, B. Moulton and M. J. Zaworotko, *Angew. Chem. Int. Ed. Engl.*, 2001, **40**, 2111–2113; B. Moulton, J. Lu, A. Mondal and M. J. Zaworotko, *Chem. Commun.*, 2001, 863–864; J. Lu, A. Mondal, B. Moulton and M. J. Zaworotko, *Angew. Chem. Int. Ed. Engl.*, 2001, **40**, 2113–2116; H. Abourahma, A. W. Coleman, B. Moulton, B. Rather, P. Shahgaldian and M. J. Zaworotko, *Chem. Commun.*, 2001, 2380–2381; B. Moulton, J. Lu, R. Hajndl, S. Hariharan and M. J. Zaworotko, *Angew. Chem. Int. Ed. Engl.*, 2002, **41**, 2821–2824; H. Abourahma, G. J. Bodwell, J. Lu, B. Moulton, I. R. Pottie, R. B. Walsh and M. J. Zaworotko, *Cryst. Growth Des.*, 2003, 513–519; B. Moulton, H. Abourahma, M. W. Bradner, J. Lu, G. J. McManus and M. J. Zaworotko, *Chem. Commun.*, 2003, 1342–1343; A. C. Sudik, A. P. Côté and O. M. Yaghi, *Inorg. Chem.*, 2005, 2998–3000; J. Zhang, Y. Kang, J. Zhang, Z.-J. Li, Y.-Y. Qin and Y.-G. Yao, *Eur. J. Inorg. Chem.*, 2006, 2253–2258; Y.-F. Zhou, F.-L. Jiang, D.-Q. Yuan, B.-L. Wu, R.-H. Wang, Z.-Z. Lin and M.-C. Hong, *Angew. Chem. Int. Ed.*, 2004, **43**, 5665–5668; A. Thirumurugan and S. Natarajan, *Cryst. Growth Des.*, 2006, 983–988; Y.-H. Wen, J. Zhang, X.-Q. Wang, Y.-L. Feng, J.-k. Cheng, Z.-J. Lia and Y.-G. Yao, *New J. Chem.*, 2005, **29**, 995–997; S. Y. Yang, L. S. Long, R. B. Huang and L. S. Zheng, *Chem. Commun.*, 2002, 472–473.
- 19 Y. Garcia, P. J. van Koningsbruggen, G. Bravic, P. Guionneau, D. Chasseau, G. L. Casciarano, J. Moscovici, K. Lambert, A. Michalowicz and O. Kahn, *Inorg. Chem.*, 1997, **36**, 6357; J.-C. Liu, D.-G. Fu, J.-Z. Zhuang, C.-Y. Duan and X.-Z. You, *J. Chem. Soc. Dalton Trans.*, 1999, 2337; P. J. Hagrman, C. Bridges, J. E. Greedan and J. Zubietta, *J. Chem. Soc. Dalton Trans.*, 1999, 2901; K. Drabent and Z. Ciunik, *Chem. Commun.*, 2001, 1254; Y. Garcia, J. Moscovici, A. Michalowicz, V. Ksenofontov, G. Levchenko, G. Bravic, D. Chasseau and P. Gütlisch, *Chem. Eur. J.*, 2002, **8**, 4992; Y. Garcia, P. J. van Koningsbruggen, G. Bravic, D. Chasseau and O. Kahn, *Eur. J. Inorg. Chem.*, 2003, 356; B. Liu, G.-C. Guo and J.-S. Huang, *J. Solid State Chem.*, 2006, **179**, 3136; B. Ding, Y. Q. Huang, Y. Y. Liu, W. Shi and P. Cheng, *Inorg. Chem. Commun.*, 2007, **10**, 7.
- 20 H. Park, D. M. Moureau and J. B. Parise, *Chem. Mater.*, 2006, **18**, 525.
- 21 L. Yi, B. Ding, B. Zhao, P. Cheng, D.-Z. Liao, S.-P. Yan and Z.-H. Jiang, *Inorg. Chem.*, 2004, **43**, 33; Y.-Q. Huang, B. Ding, H.-B. Song, B. Zhao, P. Ren, P. Cheng, H.-G. Wang, D.-Z. Liao and S.-P. Yan, *Chem. Commun.*, 2006, 4906.
- 22 G. Vos, A. J. de Kok and G. C. Verschoor, *Z. Naturforsch. B*, 1981, **36**, 809; H. Schmidbaur, A. Mair, G. Müller, J. Lachmann and S. Gamper, *Z. Naturforsch. B*, 1991, **46**, 912; O. Castillo, U. García-Couceiro, A. Luque, J. P. García-Teran and P. Roman, *Acta Cryst.*, 2004, **E60**, m9; X.-W. Liu, *Acta Cryst.*, 2005, **E61**, m1777; P. Nockemann, F. Schulz, D. Naumann and G. Meyer, *Z. Anorg. Allg. Chem.*, 2005, **631**, 649; B. Ding, L. Yi, Y. Wang, P. Cheng, D.-Z. Liao, S.-P. Yan, Z.-H. Jiang, H.-B. Song and H.-G. Wang, *Dalton Trans.*, 2006, 665; B. Liu, L. Xu, G.-C. Guo and J.-S. Huang, *J. Mol. Struct.*, 2006, **825**, 79; E. Aznar, S. Ferrer, J. Borras, F. Lloret, M. Liu-Gonzalez, H. Rodriguez-Prieto and S. Garcia-Granda, *Eur. J. Inorg. Chem.*, 2006, 5115.
- 23 A. B. Lysenko, E. V. Govor, H. Krautscheid and K. V. Domasevitch, *Dalton Trans.*, 2006, 3772; A. B. Lysenko, E. V. Govor and K. V. Domasevitch, *Inorg. Chim. Acta*, 2007, **360**, 55.
- 24  $[\text{Mn}(\text{NCS})_2(\mu\text{-btr-}\kappa\text{N1,N1'})(\text{H}_2\text{O})_2]$ : M. Biagini-Cingi, A. M. Manotti-Lanfredi, F. Uguzzoli, J. G. Haasnoot and J. Reedijk, *Gazz. Chim. Ital.*, 1994, **124**, 509.
- 25  $[\{\text{Mn}(\text{NCS})(\mu\text{-btr-}\kappa\text{N1,N1'})(\text{btr-}\kappa\text{N1})_2(\text{H}_2\text{O})\}\text{NCS}]$ : C. L. Zilverentant, W. L. Driessens, J. G. Haasnoot, J. J. A. Kolnaar and J. Reedijk, *Inorg. Chim. Acta*, 1998, **282**, 257.
- 26  $[\text{Co}(\text{NCS})_2(\mu\text{-btr-}\kappa\text{N1,N1'})]$ : W. Vreugdenhil, S. Gorter, J. G. Haasnoot and J. Reedijk, *Polyhedron*, 1985, **4**, 1769.
- 27  $[\text{Mn}(\mu\text{-N3-}\kappa\text{N1,N3})(\text{btr-}\kappa\text{N1})]$ : X.-Y. Wang, L. Wang, Z.-M. Wang, G. Su and S. Gao, *Chem. Mater.*, 2005, **17**, 6369.
- 28  $[\text{Fe}(\text{NCS})_2(\mu\text{-btr-}\kappa\text{N1,N1'})]$ : W. Vreugdenhil, J. H. van Diemen, R. A. G. de Graaff, J. G. Haasnoot, J. Reedijk, A. M. van der Kraan, O. Kahn and J. Zarembowitch, *Polyhedron*, 1990, **9**, 2971.
- 29 H. A. Habib and C. Janiak, *Acta Cryst.*, 2008, **E64**, o1199.
- 30 B. Li, Z. Xu, Z. Cao, L. Zhu and K. Yu, *Transition Met. Chem.*, 1999, **24**, 622; B. Li, J. Zou, C. Duan, Y. Liu, X. Wei and Z. Xu, *Acta Cryst.*, 1999, **C55**, 165; B. Li, B. Li, X. Zhu, L. Zhu and Y. Zhang, *Acta Cryst.*, 2003, **C59**, m350; X. Zhu, B.-Z. Li, J.-H. Zhou, B.-L. Li and Y. Zhang, *Acta Cryst.*, 2004, **C60**, m191; J. Zhou, X. Zhu, Y. Zhang, Y. Zhang and B. Li, *Inorg. Chem. Commun.*, 2004, **7**, 949; B. Li, B. Li, X. Zhu, X. Lu and Y. Zhang, *J. Coord. Chem.*, 2004, **57**, 1361; B. Li, X. Zhu, J. Zhou, Y. Peng and Y. Zhang, *Polyhedron*, 2004, **23**, 3133.
- 31 Cambridge Structure Database search, CSD Version 5.28 (November 2006) with 2 updates (January 2007, May 2007).
- 32 Y. Garcia, G. Bravic, C. Gieck, D. Chasseau, W. Tremel and P. Gütlisch, *Inorg. Chem.*, 2005, **44**, 9723.
- 33 Y. Garcia, P. J. van Koningsbruggen, H. Kooijman, A. L. Spek, J. G. Haasnoot and O. Kahn, *Eur. J. Inorg. Chem.*, 2000, 307.
- 34 F. A. A. Paz and J. Klinowski, *Inorg. Chem.*, 2004, **43**, 3882.

- 35 The Addison  $\tau$  parameter is  $\tau = 0.0$  for an ideal square pyramid and  $\tau = 1.0$  for an ideal trigonal bipyramidal; see: A. W. Addison, T. N. Rao, J. Reedijk, J. van Rijn and G. C. Verschoor, *J. Chem. Soc. Dalton Trans.*, 1984, 1349.
- 36 G. R. Desiraju and T. Steiner, The weak hydrogen bond, in: *IUCr Monograph on Crystallography*, vol. 9, Oxford Science, Oxford, 1999; G. R. Desiraju, *Acc. Chem. Res.*, 2002, **35**, 565; T. Steiner, *Chem. Commun.*, 1997, 727; G. R. Desiraju, *Acc. Chem. Res.*, 1996, **29**, 441.
- 37 C. Janiak and T. G. Scharmann, *Polyhedron*, 2003, **22**, 1123.
- 38 T. Dorn, C. Janiak and K. Abu-Shandi, *CrystEngComm*, 2005, **7**, 633–641.
- 39 C. Volkringer, D. Popon, T. Loiseau, N. Guillou, G. Férey, M. Haouas, F. Taulelle, C. Mellot-Draznieks, M. Burghammer and C. Riekel, *Nature Materials*, 2007, **6**, 760–764.
- 40 M. J. Katz, P. M. Aguiar, R. J. Batchelor, A. A. Bokov, Z.-G. Ye, S. Kroeker and D. B. Leznoff, *J. Am. Chem. Soc.*, 2006, **128**, 3669–3676.
- 41 N. Masciocchi, S. Galli, E. Alberti, A. Sironi, C. Di Nicola, C. Pettinari and L. Pandolfi, *Inorg. Chem.*, 2006, **45**, 9064–9074.
- 42 L. Ouyang, P. M. Aguiar, R. J. Batchelor, S. Kroeker and D. B. Leznoff, *Chem. Commun.*, 2006, 744–746.
- 43 R. M. Claramunt, D. Sanz, M. Pérez-Torralba, E. Pinilla, M. R. Torres and J. Elguero, *Eur. J. Org. Chem.*, 2004, 4452–4466.
- 44 H. O. Bayer, R. S. Cook, W. C. von Meyer, *U. S. Patent*, 1974, **3**, 821, 376.
- 45 STOE WinXPOW Version 1.10, STOE & Cie GmbH, Darmstadt, Germany, 2002.
- 46 APEX2 (Version 2.1-0) Data Collection Program for the CCD Area-Detector System, SAINT, *Data Reduction and Frame Integration Program for the CCD Area-Detector System*, Bruker Analytical X-ray Systems, Madison, Wisconsin, USA, 2006.
- 47 G. Sheldrick, *Program SADABS: Area-detector absorption correction*, University of Göttingen, Germany, 1996.
- 48 G. Sheldrick, *SHELXS-97, SHELXL-97, Programs for Crystal Structure Analysis*, University of Göttingen, Germany, 1997.
- 49 K. Brandenburg, Diamond (Version 3.1e), *Crystal and Molecular Structure Visualization*, Crystal Impact, K. Brandenburg, & H. Putz Gbr, Bonn, Germany, 2007.
- 50 G. Metz, M. Ziliox and S. O. Smith, *Solid State Nucl. Magn. Reson.*, 1996, **7**, 155–160; G. Metz, X. Wu and S. O. Smith, *J. Magn. Reson. A*, 1994, **110**, 219–227; G. Metz, X. Wu and S. O. Smith, *Chem. Phys. Lett.*, 1994, **173**, 461–465.
- 51 A. E. Bennett, C. M. Rienstra, M. Auger, K. V. Lakshmi and R. G. Griffin, *J. Chem. Phys.*, 1995, **103**, 6951–6958.